Dynamic Optimization-Based Control of Dextrous Manipulation

Romain Michalec **Alain Micaelli**

CEA, LIST, Interactive Simulation Laboratory
18, route du panorama, BP 6, Fontenay-aux-Roses, F-92265, France
(e-mail: romain.michalec|alain.micaelli@cea.fr)

Abstract: We present a dynamic optimization-based control for dextrous manipulation with a multi-fingered hand. The formulation of the manipulation problem as an optimization problem enables computation of the best possible control with respect to user-defined criteria, trade-off between the many different and possibly conflicting equations the hand/object system must comply with, and easy removal or addition of such equations. In this paper, control of object motion and of contact forces is provided, as well as management of non-sliding contacts, motor constraints, joint limits and articular redundancy.

Keywords: Multi-fingered hand control, quadratic programming, position/force control, optimization

1. INTRODUCTION

Because of their high versatility and their contribution to anthropomorphic identification, multi-fingered hands are choice end-effectors for humanoid robots. For instance, assistance robots for the ill, the disabled, or the elderly are intended to perform a huge variety of dexterity-demanding tasks in human-adapted environments. Therefore, it is wiser to endow them with human-like end-effectors rather than specialized grippers. The variety of tasks to be performed and the considerable amount of dexterity they require also underline the need for efficient, reliable, and versatile control structures for multi-fingered hands.

Numerous controls for dextrous, i.e. skillful, manipulation have been designed since the engineering of the first multi-fingered robot hands in the eighties (Salisbury, 1982), (Jacobsen et al., 1984). The majority of them use the equations of motion of the hand, the equations of motion of the object, and the pseudo-inverse of the grasp map to compute articular motor torques (e.g. Chen and Zribi, 2000, section 4). A drawback of this classical method is the possible non-optimality of the computed torques and articular configuration during the motion. It is also difficult to take into account multiple objectives or additional constraints, such as joint end stops or motor limitations.

It is possible to overcome these drawbacks by formulating the manipulation problem as an optimization problem constrained by the equations of motion. Additional equations are formulated into additional criteria or constraints, and optimality of multiple criteria is possible. This method may be properly described as a computed-torque method subject to criteria and constraints.

Optimization-based motion control has been first studied by (Wieber, 2000), (Collette et al., 2007), (Collette et al., 2008), (Abe et al., 2007) and (da Silva et al., 2008) for walking, standing or balance control of humanoid robots.

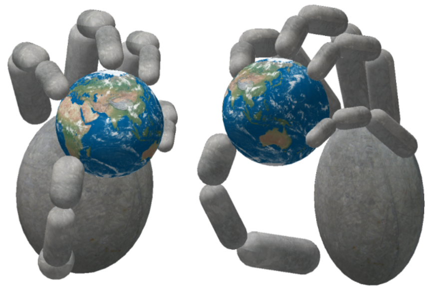

Fig. 1. Five-fingered robot hand manipulating the Earth

In computer graphics, (Liu, 2008) uses an optimization technique for hand motion synthesis, but does not compute motor torques, as control is not a CG problematic. To the best of our knowledge, optimization-based motion control of humanoids has not yet been ported, adapted and implemented in the domain of robot hand control.

This paper does this work. It presents a dynamic optimization-based control for dextrous manipulation with a multi-fingered robot hand. Control of object motion and of contact forces is provided, as well as management of non-sliding contacts, motor constraints, joint limits and articular redundancy. A complementary paper (Michalec and Micaelli, 2009) explains how to design adequate contact forces to have the grasp withstand a set of expected disturbances and achieve robust manipulation.

The formulation of the manipulation problem as an optimization problem allows for computation of the best possible control, with respect to user-defined criteria. It also enables trade-off between the different and possibly conflicting equations the hand/object system must comply with, and easy removal or addition of such equations.

The rest of this paper is as follows. The equations of the system are given in section 2, its control is presented in section 3. A simulation example is given in section 4 and section 5 concludes the paper.

2. SYSTEM KINEMATICS AND DYNAMICS

Our hand is illustrated on figure 1. It is composed of three to five anthropomorphic fingers arranged in a human-like way. Each finger is made of three phalanxes and three joints. The proximal joint has two degrees of freedom for abduction/adduction and flexion/extension.

The hand was simulated using ARBORIS, a dynamical engine for articulated rigid body mechanics created at CEA/LIST and UPMC/ISIR (Micaelli and Barthélémy, 2006). It is an open-source object-oriented toolbox for MATLAB designed with simplicity and ease-of-use in mind, allowing for control and simulation of articulated systems with numerous non-permanent contacts, especially virtual humans (Collette et al., 2007). It is targeted at rapid prototyping and benchmarking of robots and controls, human motion analysis and as an educational tool. Computer animation is not a primary goal of ARBORIS, however elaborate skinning of the skeletal animations it produces may be done with dedicated software.

All the segments in our hand are considered as rigid bodies. The root body of this tree structure, the palm, is fixed and cannot move. All the joints are torque-driven.

2.1 Basic notations and definitions

We let $n_f \geq 2$ denote the number of fingers, $n_b = 3n_f$ the number of rigid bodies (excluding the root body), and $n_{dof} = 4n_f$ the number of degrees of freedom. i and k denote respectively the indexes of a finger and a segment: $i \in [|1, n_f|]$, $k \in [|0, n_b|]$, 0 is for the palm.

Each body in the hand comes with its own frame attached at its centre of mass (figure 2). *ref* is an inertial reference frame, *root* is the frame of the palm, dp_i is the frame of the i-th distal phalanx, and *obj* is the frame of the object being manipulated. c_i denotes both the contact point between the object and the i-th distal phalanx and the contact frame $(\boldsymbol{t}_i^1, \boldsymbol{t}_i^2, \boldsymbol{n}_i)$, with $\boldsymbol{n}_i$ outward and normal to the object's surface (figure 2).

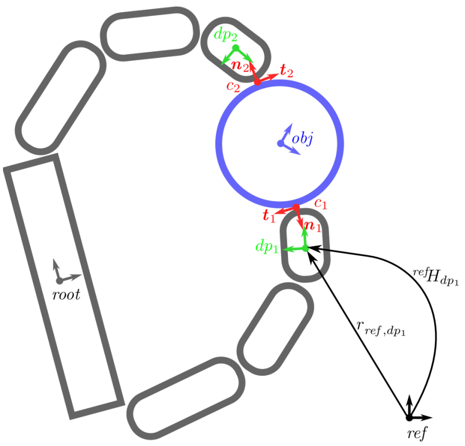

Fig. 2. Frames and homogeneous transforms

Each body is located through a homogeneous transform between the inertial frame and its own frame. For instance:

$$^{ref}H_{dp_i} = \begin{pmatrix} ^{ref}R_{dp_i} & r^{ref}_{ref,dp_i} \\ 0_{1,3} & 1 \end{pmatrix} \in SE_3(\mathbb{R})$$

locates the i-th distal phalanx relatively to *ref* through the rotation $^{ref}R_{dp_i} \in SO_3(\mathbb{R})$ between the bases of the frames and the translation $r^{ref}_{ref,dp_i} \in \mathbb{R}^3$ from the origin of *ref* to the origin of dp_i, this vector being written in *ref* coordinates (figure 2).

The mass and inertia of body k are arranged into the body's generalized mass matrix: $M_k = \text{diag}\,(m_k I_3, [I]_k)$, where m_k is the mass of body k and $[I]_k$ is its inertia tensor written in its own frame.

$q = (q_1, \dots, q_{n_{dof}})^T$ denotes the column vector of articular coordinates and $\tau = (\tau_1, \dots, \tau_{n_{dof}})^T$ denotes the column vector of driving torques.

2.2 Hand kinematics

We let V_k denote the twist of body k, written in the own frame of body k. That is to say:

$$V_k = \begin{pmatrix} v_k = v^k_{k/ref} \\ \omega_k = \omega^k_{k/ref} \end{pmatrix}$$

with v_k the velocity of the center of mass of body k and ω_k the angular velocity of body k, both relative to the reference frame and written in the frame of body k. All velocities from now on are *absolute* (relative to the reference frame) but written in the adequate body frame, except if stated otherwise.

We may write the direct kinematic model as:

$$V_k = \tilde{J}_k\, \tilde{\dot{q}} = J_k\, \dot{q}$$

with $\tilde{\dot{q}}$ the subset of $\dot{q}$ involved in the kinematic chain between the palm and k-th body, $\tilde{J}_k$ the jacobian of this chain, and J_k being obtained from $\tilde{J}_k$ by padding with zeros where appropriate. Then we stack all the V_k and J_k together and get:

$$V = J\,T \tag{1}$$

$$V = \begin{pmatrix} V_{root} \\ V_1 \\ \vdots \\ V_{n_b} \end{pmatrix} \qquad J = \begin{pmatrix} J_{root} \\ J_1 \\ \vdots \\ J_{n_b} \end{pmatrix} \qquad T = \begin{pmatrix} V_{root} \\ \dot{q}_1 \\ \vdots \\ \dot{q}_{n_{dof}} \end{pmatrix}$$

The resulting $(6 + 6n_b, n_{dof})$ jacobian matrix maps the joint velocity space into the body twist space $se_3(\mathbb{R})^{1+n_b}$.

2.3 Contact modeling

Contacts between the distal phalanxes and the object are modeled as rigid point contacts with friction. The forces $f_i \in \mathbb{R}^3$ applied by the fingers on the object are assumed written in their respective contact frames c_i.

A first constraint on the contact force f_i is that it must remain unilateral: $(f_i)_n \leq 0$. The notation $()_n$ is for the normal component; $()_t$ will denote the tangential one.

A second constraint results from the Coulomb friction conditions. They state that no sliding of the contact occurs if $||(f_i)_t|| \leq \mu||(f_i)_n||$ (figure 3). μ denotes the dry friction coefficient; we assume that the static and dynamic coefficients are equal.

It is well-known that the Coulomb non-sliding condition may be linearized by approximating the contact cone with a multi-faceted cone (figure 3), and that the resulting linear constraint also accounts for unilaterality. That is, if we define $f = (f_1, \dots, f_{n_f})^T$ the column vector of all the

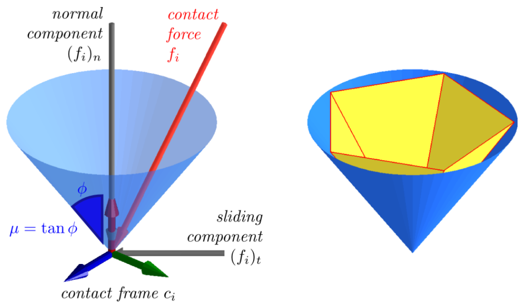

Fig. 3. A non-sliding contact, its exact and linearized cones

contact forces, we may find matrices C and d such that all the non-sliding and unilaterality constraints read:

$$C f + d \leq 0_{n_f \times n_e, 1} \tag{2}$$

C is $(n_f \times n_e, 3n_f)$, n_e being the number of edges in the cone discretization; d is a column vector with $n_f \times n_e$ lines.

2.4 Hand dynamics

The hand dynamics is the usual inverse dynamic model for robot manipulators:

$$J^T M J \, (\dot{T} - \mathcal{G}) + NT - J^T W_{hand} = L\,\tau \tag{3}$$

In this system of $6 + n_{dof}$ equations, J is the jacobian defined in (1), NT are the inertial and Coriolis forces, $\mathcal{G}$ is for gravity, W_{hand} denotes external wrenches that may be applied on the hand's segments:

$$M = \begin{pmatrix} M_{root} & & & \\ & M_1 & & \\ & & \ddots & \\ & & & M_{n_b} \end{pmatrix} \quad W_{hand} = \begin{pmatrix} W_{root} \\ W_1 \\ \vdots \\ W_{n_b} \end{pmatrix} \quad L = \begin{pmatrix} 0_{6,n_{dof}} \\ I_{n_{dof}} \end{pmatrix}$$

$$\mathcal{G} = \begin{pmatrix} 0 & 0 & -\tilde{g} \mid 0_{1,3} \mid 0_{1,n_{dof}} \end{pmatrix}^T \qquad \tilde{g} = \text{gravity intensity}$$

Each W_k denotes the external wrench applied on body k, written in the own frame of body k. That is to say:

$$W_k = \begin{pmatrix} f_k = f^k_{ext \to k} \\ m_k = m^k_{ext \to k} \end{pmatrix}$$

with f_k the force applied on body k and m_k the moment of this force at the center of mass of body k, both written in the frame of body k. From now on, all wrenches are written in their appropriate body frame, except if stated otherwise.

From a control point of view, most W_k are zero, except W_{dp_i} that are the contact wrenches resulting from the forces $-f_1, \ldots, -f_{n_f}$ applied by the object on the fingers.

2.5 Relation between contact forces and object motion

The object motion is the result of contact and gravity forces. Disturbances may also happen but are unknown to the controller. From a control perspective the object dynamics is:

$$M_{obj} \, (\dot{V}_{obj} - g) + N_{obj} V_{obj} = W_{dp \to obj} \tag{4}$$

where all quantities are written in the object frame. In particular, the gravity wrench $M_{obj}\, g$ and the resultant wrench applied by the fingers on the object are:

$$M_{obj}\, g \overset{\text{def}}{=} \begin{pmatrix} m_{obj} I_3 & 0_{3,3} \\ 0_{3,3} & [I]_{obj} \end{pmatrix} \begin{pmatrix} {}^{obj}R_{ref} \begin{pmatrix} 0 \\ 0 \\ -\tilde{g} \end{pmatrix} \\ 0_{3,1} \end{pmatrix} = m_{obj}\, g \tag{5}$$

$$W_{dp \to obj} = \sum_{i=1}^{n_f} {}^{obj}Ad_{c_i}^{-T} \, W_{dp_i \to obj} \tag{6}$$

where ${}^{obj}Ad_{c_i}^{-T}$ is the co-adjoint matrix of ${}^{obj}H_{c_i}$ and $W_{dp_i \to obj}$ is the wrench applied by finger i:

$${}^{obj}Ad_{c_i}^{-T} = \begin{pmatrix} {}^{obj}R_{c_i} & 0_{3,3} \\ \hat{r}^{obj}_{obj,c_i} \, {}^{obj}R_{c_i} & {}^{obj}R_{c_i} \end{pmatrix} \qquad W_{dp_i \to obj} = \begin{pmatrix} f_i \\ 0_{3,1} \end{pmatrix}$$

with $\hat{}$ denoting the operation that returns a skew-symmetric matrix for cross-product by the input vector: $\hat{\boldsymbol{r}}\boldsymbol{u} = \boldsymbol{r} \times \boldsymbol{u}$. In the end, we get:

$$W_{dp \to obj} = \begin{pmatrix} {}^{obj}R_{c_1} & \ldots & {}^{obj}R_{c_{n_f}} \\ \hat{r}^{obj}_{obj,c_1} \, {}^{obj}R_{c_1} & \ldots & \hat{r}^{obj}_{obj,c_{n_f}} \, {}^{obj}R_{c_{n_f}} \end{pmatrix} \begin{pmatrix} f_1 \\ \vdots \\ f_{n_f} \end{pmatrix} \overset{\text{def}}{=} G\, f \tag{7}$$

This matrix G is called the *grasp map* of the grip.

2.6 Joint constraints

Actuators are not infinitely powerful. We must compute the control torques according to the following constraints:

$$\tau_{min} \leq \tau \leq \tau_{max} \tag{8}$$

Robot joints have end stops. We make the control aware of these limits so that it does not try to break them. We integrate the articular acceleration using backward Euler integration: $\dot{q}_t = \dot{q}_{t-dt} + \ddot{q}_t dt$ and $q_t = q_{t-dt} + \dot{q}_t dt$. With these two equations we get: $q_t = q_{t-dt} + \dot{q}_{t-dt} dt + \ddot{q}_t dt^2$.

Therefore do constraints on q_t result in constraints on $\ddot{q}_t$:

$$q_{min} \leq q_t \leq q_{max} \Rightarrow$$

$$\frac{(q_{min} - q_{t-dt} - \dot{q}_{t-dt} dt)}{dt^2} \leq \ddot{q}_t \leq \frac{(q_{max} - q_{t-dt} - \dot{q}_{t-dt} dt)}{dt^2}$$

The resulting constraints have the following form:

$$\ddot{q}_{min}(q_{t-dt}, \dot{q}_{t-dt}) \leq L^T \dot{T}_t \leq \ddot{q}_{max}(q_{t-dt}, \dot{q}_{t-dt}) \tag{9}$$

3. DYNAMIC OPTIMIZATION-BASED CONTROL

In the previous section, we list several equations that the hand/object system must absolutely meet. For instance, consistency of the control torques with the dynamic model (3) is such an equation, and the most important.

The *constraints* we enumerated are summarized in table 1, together with the unknowns they are relative to.

Table 1. Constraints and their unknowns

	Constraint	Unknowns
(2)	$C f + d \leq 0_{n_f \times n_e, 1}$	f
(3)	$J^T M J \, (\dot{T} - \mathcal{G}) + NT - J^T W_{hand} = L\,\tau$	$\dot{T}$, f, τ
(8)	$\tau_{min} \leq \tau \leq \tau_{max}$	τ
(9)	$\ddot{q}_{min}(q_{t-dt}, \dot{q}_{t-dt}) \leq L^T \dot{T}_t \leq \ddot{q}_{max}(q_{t-dt}, \dot{q}_{t-dt})$	$\dot{T}$

Other equations the hand/object system need not meet perfectly, but should comply with to the best of its abilities, are *criteria* to optimize. Objectives are such equations, as they are not always guaranteed to be feasible.

Eventually the control problem may be written as a constrained optimization problem:

$$\begin{cases} \text{optimize } \textit{criteria} \\ \text{with respect to the variables } \tau,\ \dot{T},\ f \\ \text{and subject to the } \textit{constraints} \text{ (2), (3), (8), (9)} \end{cases} \tag{10}$$

The resulting optimal τ is the vector of control torques at the current time. The following subsections present the equations that form the criteria to optimize.

3.1 Desired object motion

Equation (4) shows that the object motion $\dot{V}_{obj}$ must be controlled through $W_{dp \to obj}$, i.e. through the contact forces f. That is to say, a user-specified high-level objective on $\dot{V}_{obj}$ induces a lower-level objective on the variable f.

We let ${}^{root}H_{obj}^{[d]} \in SE_3(\mathbb{R})$ and $V_{obj/root}^{[d]} \in se_3(\mathbb{R})$ denote desired trajectories for the object, respectively in position and orientation and in linear and angular velocities. Both are relative to the palm, as it is a natural reference frame for object manipulation.

We have the following expressions for the quantities to control, and the same expressions with a $[d]$ superscript for their desired values:

$$ {}^{root}H_{obj} = \begin{pmatrix} {}^{root}R_{obj} & r_{root,obj}^{root} \\ 0_{3,1} & 1 \end{pmatrix} \qquad V_{obj/root} = \begin{pmatrix} v_{obj/root}^{obj} \\ \omega_{obj/root}^{obj} \end{pmatrix} $$

The errors are as follows, all written in obj coordinates:

$$ \begin{aligned} \varepsilon_x &= {}^{obj}R_{root}\,(r_{root,obj}^{root,[d]} - r_{root,obj}^{root}) \\ \varepsilon_R &= [\mathrm{skew}\,({}^{root}R_{obj}^{T}\;{}^{root}R_{obj}^{[d]})]^{\vee} \\ \varepsilon_v &= v_{obj/root}^{obj,[d]} - v_{obj/root}^{obj} \\ \varepsilon_\omega &= \omega_{obj/root}^{obj,[d]} - \omega_{obj/root}^{obj} \end{aligned} \tag{11} $$

with skew () denoting the skew-symmetric part of a matrix and $^{\vee}$ being the operation that returns a vector for cross-product from a skew-symmetric matrix.

We use these errors to design a proportional-derivative corrective action for the object motion $\dot{V}_{obj/root}$, and since $V_{obj/root} = V_{obj}$ because we assumed that the palm does not move, we write:

$$ \dot{V}_{obj}^{[d]} = \dot{V}_{obj/root}^{[d]} = \begin{pmatrix} k_x\,\varepsilon_x + k_v\,\varepsilon_v \\ k_R\,\varepsilon_R + k_\omega\,\varepsilon_\omega \end{pmatrix} \tag{12} $$

The gain matrices k_x, k_R, k_v and k_ω are $(3,3)$ diagonal matrices whose coefficients have effect on the obj coordinates of the errors.

Using (4) and (12), we get the following expression of the wrench that should be applied on the object:

$$ W_{dp \to obj}^{[d]} = M_{obj}\,(\dot{V}_{obj}^{[d]} - g) + N_{obj} V_{obj} \tag{13} $$

In our optimization problem (10), we minimize the difference between the wrench that should be applied and the wrench that may be applied considering the constraint equations. Hence the following optimization criteria:

$$ \begin{aligned} &\min_f \frac{1}{2} \|W_{dp \to obj}^{[d]} - W_{dp \to obj}\|_{Q_W}^2 \\ &= \min_f \left[\frac{1}{2} W_{dp \to obj}^T Q_W W_{dp \to obj} + W_{dp \to obj}^T r_W \right] \end{aligned} \tag{14} $$

with $r_W = -Q_W W_{dp \to obj}^{[d]}$ and Q_W a weight matrix for this criteria (symmetric positive-definite matrix). Eventually we use (7) and (14) and get this criteria:

$$ \begin{aligned} &\min_f \frac{1}{2} \|W_{dp \to obj}^{[d]} - W_{dp \to obj}\|_{Q_W}^2 \\ &= \min_f \left[\frac{1}{2} f^T Q_{obj} f + f^T r_{obj} \right] \end{aligned} \tag{15} $$

with $Q_{obj} = G^T Q_W G$, $r_{obj} = G^T r_W = -G^T Q_W W_{dp \to obj}^{[d]}$.

3.2 Other objectives about the contact forces

It may be that the desired object motion is not the only objective on the contact force variable f. Usually, we also want the hand to apply a certain amount of squeezing on the object, especially to resist potential disturbances.

Basic squeezing can be achieved by specifying an adequate normal objective: $f^{[d]} = (0, 0, (f_1)_n^{[d]}, \ldots, 0, 0, (f_{n_f})_n^{[d]})^T$. The corresponding criteria is:

$$ \min_f \frac{1}{2} \|f^{[d]} - f\|_{Q'_f}^2 = \min_f \left[\frac{1}{2} f^T Q'_f f + f^T r'_f \right] \tag{16} $$

with $r'_f = -Q'_f f^{[d]}$. Careful choice of the Q'_f weight matrix is the key to take the best advantage of the trade-off nature of the optimization. First, it should not outweight Q_{obj} for the manipulation to be considered as prioritary upon the tightening. Second, the coefficients in Q'_f relative to the zeros in $f^{[d]}$ should be much smaller than those relative to the $(f_i)_n$, because these zeros are bogus objectives (the criteria lays on $(f)_n$, not on $(f)_t$) that could interfere with the other objectives if not non-prioritary.

An asset of this method is that the objective is easy to design, but a drawback is that it is not neutral with respect to the object static equilibrium. Indeed, in most finger configurations, such normal contact forces induce a non-zero, unmodelled wrench on the object, prone to hinder the manipulation task.

A much proper method of specifying a tightening task is through a global desired robustness, i.e. we keep criteria (16) but design $f^{[d]}$ in a better way: see (Michalec and Micaelli, 2009).

3.3 Non-sliding objective

Non-sliding contacts are characterized by the nullity of their sliding velocity: $v_s = v_{c_i \in dp_i/obj} = 0_{3,1}$.

We should provide for the satisfaction of this equation through a constraint on the contact acceleration, which would induce a constraint on the joint accelerations $\dot{T}$. But this would be too restrictive a constraint and (10) could become over-constrained. We rather write an objective on the contact acceleration, resulting in a criteria on $\dot{T}$.

We let $c_i \in obj$ denote the i-th contact point on the object and $c_i \in dp_i$ denote the same contact point, but on dp_i. Both points are at the same place, but may have different velocities, and the sliding velocity is this difference: $v_s = v_{c_i \in dp_i/obj} = v_{c_i \in dp_i} - v_{c_i \in obj}$.

We control $c_i \in dp_i$ to limit sliding through the following objective: $v_{c_i \in dp_i}^{[d]} = v_{c_i \in obj}$. In this way, we make sure that the error $\varepsilon_s = v_{c_i \in dp_i}^{[d]} - v_{c_i \in dp_i} = -v_s$ is minimized. We use a simple derivative correction: $\dot{v}_{c_i \in dp_i}^{[d]} = k_s\,\varepsilon_s = k_s\,(v_{c_i \in dp_i}^{[d]} - v_{c_i \in dp_i})$.

It is only a matter of adjoint matrices and of using (1) to prove that $v_{c_i \in dp_i}^{[d]} = \Pi\,{}^{c_i}Ad_{obj} V_{obj}$ and that $v_{c_i \in dp_i} = \Pi\,{}^{c_i}Ad_{dp_i} V_{dp_i} = \Pi\,{}^{c_i}Ad_{dp_i} J_{dp_i} T$, with $\Pi = (I_3\ 0_{3,3})$. Thus $\dot{v}_{c_i \in dp_i}^{[d]} = k_s\,(\Pi\,{}^{c_i}Ad_{obj} V_{obj} - \Pi\,{}^{c_i}Ad_{dp_i} J_{dp_i} T)$.

Derivation of the expression of $\dot{v}_{c_i \in dp_i}$ yields:

$$\dot{v}_{c_i \in dp_i} = \Pi\, {}^{c_i}\!Ad_{dp_i} J_{dp_i} \dot{T} + \Pi\, {}^{c_i}\!Ad_{dp_i} \dot{J}_{dp_i} T \overset{\text{def}}{=} F\dot{T} + \dot{F}\,T$$

We do not take ${}^{c_i}\!\dot{Ad}_{dp_i}$ into account because $c_i \in dp_i$ is supposed fixed on dp_i.

In the end, the criteria is:

$$\begin{aligned} \min_{\dot{T}} \frac{1}{2} ||\dot{v}^{[d]}_{c_i \in dp_i} - \dot{v}_{c_i \in dp_i}||^2_{Q_{c_i}} \\ = \min_{\dot{T}} \left[\frac{1}{2} \dot{T}^T Q_s \dot{T} + \dot{T}^T r_s \right] \end{aligned} \quad (17)$$

with $Q_s = F^T Q_{c_i} F$ and $r_s = F^T Q_{c_i} (\dot{F}\,T - \dot{v}^{[d]}_{c_i \in dp_i})$.

This criteria is for one non-sliding contact only; we may get a similar criteria relative to all the contacts, and similar Q_s and r_s, by concatenating adequately vectors and matrices.

3.4 Other objectives

Among all motor torques τ that satisfy the previous constraints and objectives, reason tells to choose the smallest for motor's sake. Hence $\tau^{[d]} = 0_{n_{dof},1}$ and:

$$\min_{\tau} \frac{1}{2} ||\tau^{[d]} - \tau||^2_{Q_\tau} = \min_{\tau} \left[\frac{1}{2} \tau^T Q_\tau \tau + \tau^T r_\tau \right] \quad (18)$$

where Q_τ is an non-prioritary weight matrix and $r_\tau = -Q_\tau \tau^{[d]} = 0_{n_{dof},1}$.

Control computation should also take into account the physiological coupling between the distal and intermediate phalanxes: the former's articular coordinate is partially set by the latter's. The coupling is usually considered as almost linear, and constraints between $q_{dist} = \frac{2}{3} q_{mid}$ (Rijpkema and Girard, 1991) and $q_{dist} = q_{mid}$ (Biagiotti et al., 2003) are of common use. It is better to make this coupling an objective rather than a constraint as it has anatomical precision: fairly large errors are accepted.

We use a simple articular proportional-derivative corrective action with desired values $q^{[d]}_{dist} = q_{mid}$ and $\dot{q}^{[d]}_{dist} = 0$:

$$\ddot{q}^{[d]}_{dist} = k_{q_{dist}} \left(q^{[d]}_{dist} - q_{dist}\right) + k_{\dot{q}_{dist}} \left(\dot{q}^{[d]}_{dist} - \dot{q}_{dist}\right)$$

Then we define the objectives $\ddot{q}^{[d]}_{other} = 0$ as we did for the desired contact forces in (16), concatenate those objectives, define an adequate weight matrix Q_q and write:

$$\min_{\dot{T}} \frac{1}{2} ||\ddot{q}^{[d]} - L^T\, \dot{T}||^2_{Q_q} = \min_{\dot{T}} \left[\frac{1}{2} \dot{T}^T Q'_{\dot{T}} \dot{T} + \dot{T}^T r'_{\dot{T}} \right] \quad (19)$$

with $Q'_{\dot{T}} = L\, Q_q\, L^T$ and $r'_{\dot{T}} = -L\, Q_q\, \ddot{q}^{[d]}$.

This last criteria is important because it helps manage the redundancy of the finger kinematic chains. It improves the visual realism of the grasp by limiting unusual, unanatomical joint configurations, without totally reducing finger redundancy.

3.5 Summary

We end up with the criteria summarized in table 2.

We define the unknown $y = (\tau, \dot{T}, f)^T$ and the matrices:

$$Q = \begin{pmatrix} Q_\tau & & \\ & Q_{\dot{T}} = Q_s + Q'_{\dot{T}} & \\ & & Q_f = Q_{obj} + Q'_f \end{pmatrix} \qquad r = \begin{pmatrix} r_\tau \\ r_{\dot{T}} = r_s + r'_{\dot{T}} \\ r_f = r_{obj} + r'_f \end{pmatrix}$$

Table 2. Criteria and their unknowns

	Objective	Criteria	Unknowns
(15)	$W^{[d]}_{dp \to obj}, Q_W$	$\to \min_f \left[\frac{1}{2} f^T Q_{obj} f + f^T r_{obj}\right]$	f
(16)	$f^{[d]}, Q'_f$	$\to \min_f \left[\frac{1}{2} f^T Q'_f f + f^T r'_f\right]$	f
(17)	$\dot{v}^{[d]}_{c_i \in dp_i}, Q_{c_i}$	$\to \min_{\dot{T}} \left[\frac{1}{2} \dot{T}^T Q_s \dot{T} + \dot{T}^T r_s\right]$	$\dot{T}$
(18)	$\tau^{[d]}, Q_\tau$	$\to \min_\tau \left[\frac{1}{2} \tau^T Q_\tau \tau + \tau^T r_\tau\right]$	τ
(19)	$\ddot{q}^{[d]}, Q_q$	$\to \min_{\dot{T}} \left[\frac{1}{2} \dot{T}^T Q'_{\dot{T}} \dot{T} + \dot{T}^T r'_{\dot{T}}\right]$	$\dot{T}$

We also define A_{eq}, b_{eq}, A_{neq} and b_{neq} such that (2), (3), (8), and (9) end up as $A_{eq}\, y + b_{eq} = 0$ and $A_{neq}\, y + b_{neq} \leq 0$. Eventually, the optimization-based control computation is:

$$\begin{cases} \min_y \frac{1}{2} y^T Q y + y^T r \\ A_{eq}\, y + b_{eq} = 0 \\ A_{neq}\, y + b_{neq} \leq 0 \end{cases} \quad (20)$$

This constrained quadratic programming problem may be solved using a variety of algorithms. From its solution y^{sol} we get τ^{sol}, the optimal control torques that comply with all the constraints and criteria.

4. A SIMULATION EXAMPLE

In this section, we demonstrate the use of our control in a simple manipulation task involving translation and rotation of a spherical object by a four-fingered hand.

The desired motion is illustrated on figure 4. It is made of three parts. During the first part, from 1 s to 2 s, the desired motion is set to the initial position of the object. From 2 s to 3 s, it is made of a rotation of 45° around the object's y axis in 0.5 s and of a translation of 2 cm along the same y axis in 1 s. From 2 s to 3 s, it is at rest again.

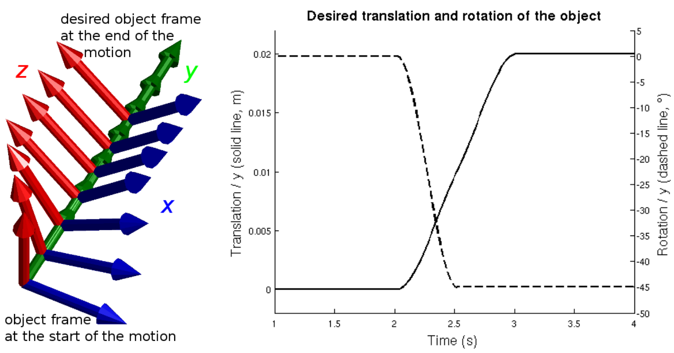

Fig. 4. Desired motion for the object body frame

The time gap from 0 s to 1 s is for the hand to set contact on the object. Its initial articular posture encircles the object and contact is set through proportional-derivative control of the end of the distal phalanxes. This control is itself embedded as a criteria in a simplified and adapted version of our optimization-based control.

A contact force objective accounts for light squeezing of the object with normal forces $(f_i)^{[d]}_n = 0.5$ N $\forall\, i \in [|1, 4|]$: see (16), section 3.2. As we explained in this section, choosing a larger objective for more tightening may hinder motion control. For the same reason, the priority of this objective is well below the priority of the desired object motion: we set $Q'_f = 10\, I_{3n_f} \ll Q_W = 10000\, I_6$.

All the weight matrices we use are diagonal for convenience (table 3). Gravity is set to zero and we use $n_e = 8$ and $\mu = 0.8$ for all the contacts. Figure 5 illustrates the resulting tracking of the desired trajectory. Errors are small and are the result of our controller's design to try and satisfy multiple objectives and multiple constraints.

Table 3. Weight matrices for the criteria

(15)	object motion	$Q_W = 10000\, I_6$
(16)	object tightening	$Q'_f = 10\, I_{3n_f}$
(17)	non-sliding contacts	$Q_{c_i} = 10000\, I_{3n_c}$
(18)	minimal motor torques	$Q_\tau = 1\, I_{n_{dof}}$
(19)	coupling of distal and middle joints	$Q_q = 1000\, I_{n_{dof}}$

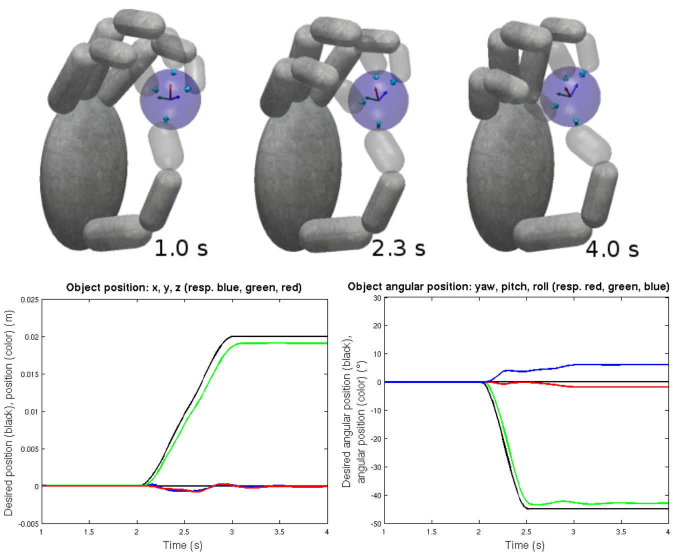

Fig. 5. Tracking of the object desired trajectory

Figure 6 illustrates the trade-off nature of this control: the same manipulation was executed at $Q_W = 1000\, I_6$ and $Q'_f = 3000\, I_{3n_f}$ for more tightening. As a result, the manipulation task is impaired. As we already mentionned, this is not a correct way to take robustness into account.

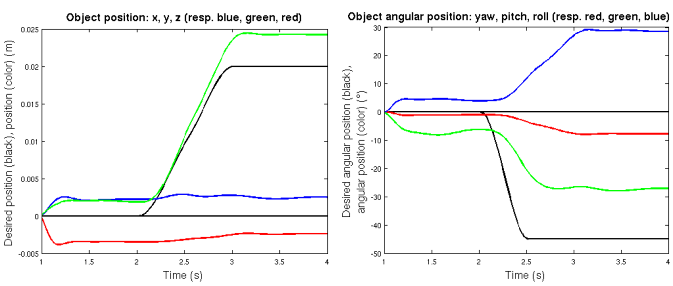

Fig. 6. A bad choice of weight matrices impairs tracking

5. CONCLUSION

In this paper, we proposed a dynamic optimization-based control for dextrous manipulation inspired by the work of (Collette et al., 2007) and (Abe et al., 2007) on humanoid motion control. The method is best described as computed torque with constraints and criteria. It allows for trade-off between the different objectives and constraints, and is easily adaptable through addition or removal of such equations, or adjustment of weight matrices.

For instance, it is possible to endow the grasp with robustness abilities in face of possible disturbances through properly-designed contact force objectives. In (Michalec and Micaelli, 2009), we compute pre-strain forces providing direction-independant robustness for the grasp.

Future work includes optimization-based control of palm motion and sliding contacts. Palm usage enlarges the motion range of feasible manipulations. Controlled slip is of such a constant use in our everyday manipulations, especially during grasp reconfigurations, that any dextrous control should account for it. However there are few studies addressing this aspect of dextrous manipulation.

ACKNOWLEDGEMENTS

The authors would like to thank Cyrille Collette (CEA, LIST) and Sébastien Barthélémy (UPMC, ISIR).

REFERENCES

Abe, Y., da Silva, M., and Popović, J. (2007). Multiobjective control with frictional contacts. In *ACM SIGGRAPH/EG Symp. Computer Animation*, 249–258.

Biagiotti, L., Liu, H., Hirzinger, G., and Melchiorri, C. (2003). Cartesian impedance control for dextrous manipulation. In *IEEE/RSJ Int. Conf. Intelligent RObots and Systems*, 3270–3275.

Chen, J. and Zribi, M. (2000). Control of multi-fingered robot hands with rolling and sliding contacts. *Int. Journal Advanced Manufacturing Technology*, 16, 71–77.

Collette, C., Micaelli, A., Lemerle, P., and Andriot, C. (2007). Dynamic balance control of humanoids for multiple grasps and non coplanar frictional contacts. In *IEEE-RAS Int. Conf. Humanoid Robots*.

Collette, C., Micaelli, A., Lemerle, P., and Andriot, C. (2008). Robust balance optimization control of humanoid robots with multiple non coplanar grasps and frictional contacts. In *IEEE Int. Conf. Robotics and Automation*, 3187–3193.

da Silva, M., Abe, Y., and Popović, J. (2008). Interactive simulation of stylized human locomotion. In *ACM SIGGRAPH papers*, 82:1–82:10.

Jacobsen, S.C., Wood, J.E., Knutti, D.F., and Biggers, K.B. (1984). The Utah/MIT dextrous hand: work in progress. *Int. Journal Robotics Research*, 3(4), 21–50.

Liu, C.K. (2008). Synthesis of interactive hand manipulation. In *ACM SIGGRAPH/EG Symp. Computer Animation*, 163–171.

Micaelli, A. and Barthélémy, S. (2006). Arboris. `https://vizir.robot.jussieu.fr/trac/arboris`.

Michalec, R. and Micaelli, A. (2009). Optimal tightening forces for multi-fingered robust manipulation. In *IEEE/RSJ Int. Conf. Intelligent RObots and Systems*.

Rijpkema, H. and Girard, M. (1991). Computer animation of knowledge-based human grasping. *ACM SIGGRAPH Computer Graphics*, 25(4), 339–348.

Salisbury, J.K. (1982). *Kinematic and force analysis of articulated hands*. Ph.D. thesis, Stanford University, Dept. Mech. Eng., Stanford, CA, USA.

Wieber, P.B. (2000). *Modélisation et commande d'un robot marcheur anthropomorphe*. Ph.D. thesis, École nationale supérieure des Mines de Paris, Paris, France.